ResearchGate

See discussions, stats, and author profiles for this publication at: https://www.researchgate.net/publication/263940926

Inhibition of Asphaltene Precipitation by TiO2, SiO2, and ZrO2 Nanofluids

ARTICLE *in* ENERGY & FUELS · JUNE 2011

Impact Factor: 2.79 · DOI: 10.1021/ef2001635

CITATIONS
16

READS
194

6 AUTHORS, INCLUDING:

Zahra Fakhroueian
University of Tehran
25 PUBLICATIONS **109** CITATIONS
SEE PROFILE

Alireza Bahramian
University of Tehran
44 PUBLICATIONS **252** CITATIONS
SEE PROFILE

Reza Azin
Persian Gulf University
54 PUBLICATIONS **184** CITATIONS
SEE PROFILE

Available from: Reza Azin
Retrieved on: 01 February 2016

energy&fuels

ARTICLE

pubs.acs.org/EF

Inhibition of Asphaltene Precipitation by TiO_2, SiO_2, and ZrO_2 Nanofluids

Mohsen Mohammadi,[†] Mahdi Akbari,[†] Zahra Fakhroueian,[‡] Alireza Bahramian,[‡,*] Reza Azin,[§] and Sharareh Arya[⊥]

[†]School of Chemical Engineering, University of Tehran, Tehran, Iran

[‡]Institute of Petroleum Engineering, P.O. Box: 11155-4563, University of Tehran, Iran

[§]Department of Chemical Engineering, School of Engineering, Persian Gulf University, Bushehr 7516913798, Iran

[⊥]NIOC-R&D, Negar St., Valiasr St., Tehran, Iran

ABSTRACT: Asphaltene precipitation causes several problems during crude oil production, transportation, and refinery processes. Therefore, finding an inhibitor to prevent or delay asphaltene precipitation is of paramount importance. In this work, effects of TiO_2, ZrO_2, and SiO_2 fine nanoparticles in organic-based nanofluids have been investigated to study their potential for stabilizing asphaltene particles in oil. To this end, polarized light microscopy has been applied to determine the onset of asphaltene precipitation by titration of dead oil samples from Iranian crude oil reservoirs with *n*-heptane in the presence of nanofluids. Results show that rutile (TiO_2) fine nanoparticles can effectively enhance the asphaltene stability in acidic conditions and act inversely in basic conditions. It was found that the required amount of *n*-heptane for destabilizing the colloidal asphaltene is considerably higher in presence of TiO_2 nanofluids at pH below 4. The FTIR spectroscopy indicates changes in *n*-heptane insoluble asphaltene when acidic TiO_2 nanofluid is used as inhibitor. According to the results obtained by FTIR spectroscopy, TiO_2 nanoparticles can enhance the stability of asphaltene nanoaggregates through formation of hydrogen bond at acidic conditions. This is while other materials used in this experiment, as well as the TiO_2 nanoparticles in basic conditions, are unable to form any hydrogen bond — hence their incapability to prevent asphaltene precipitation. Dynamic light scattering (DLS) measurements also have been performed to explain the mechanism of asphaltene precipitation in the presence of nanoparticles.

1. INTRODUCTION

Asphaltene is one of the heaviest and most polar fractions of the reservoir oil, known as the fraction soluble in aromatic solvents such as toluene and xylene but insoluble in light alkanes such as *n*-pentane and *n*-heptane.[1,2] Asphaltene exists in equilibrium with other constituents of crude oil at certain reservoir conditions. Any change in equilibrium conditions, such as pressure, temperature, or oil composition can lead to aggregation and precipitation of asphaltene particles out of crude oil.[2] The precipitated asphaltene causes many problems in production process by plugging equipments and wellbore tubing.[3,4] There are two general methods for dealing with this problem, that is removal of deposited asphaltene or inhibition of its precipitation. Dissolving deposited asphaltene by solvent and mechanical treatment are common ways for removing precipitated asphaltene. These cleanup techniques are costly and time-consuming. The second method involves stabilizing asphaltene in oil and delaying its precipitation. For this purpose, many researches[5−8] have been conducted to find suitable chemicals that can inhibit or postpone precipitation process. Amphiphiles are famous examples of inhibitors suggested to inhibit the phase separation of asphaltene from oil or disperse asphaltene particles in oil.[9−13] One of the main reasons for their effect on inhibition is the interaction between these materials and asphaltene because of their polarity.[14]

Nanofluids are suspensions containing nanoparticles with sizes mostly smaller than 100 nm. The surface charge of nanoparticles can be adjusted with pH. As already mentioned, the polarity of inhibitors is very effective on stability of asphaltene; therefore, it may be possible to stabilize the asphaltene particles by adjusting the surface charge of nanoparticles added to the oil. According to DLVO theory,[15] the asphaltene polarity and nanoparticles surface charge provide interaction between asphaltene and nanoparticles.

However, effectiveness of nanoparticles on rock wettability alteration and Enhanced Oil Recovery (EOR) has recently been addressed.[16−18] It has been suggested that adding nanoparticles to the injecting fluid can enhance the oil recovery by altering the wettability pattern of reservoir rock or changing the reservoir fluid properties. This article reveals that nanoparticles may also serve as inhibitors for asphaltene precipitation. The next sections comprise the results of some experimental tests that are designed to investigate the effects of three nanoparticles (TiO_2, SiO_2, and ZrO_2) on asphaltene precipitation. The nanoparticles are synthesized through a sol−gel method. As supporting experiment, they have been employed in an oil titration method, making use of the polarized light microscopy technique, to check their potential in stabilizing or destabilizing asphaltene nanoaggregates.

Received: January 29, 2011
Revised: June 17, 2011
Published: June 18, 2011

ACS Publications © 2011 American Chemical Society

2. EXPERIMENTAL SECTION

2.1. Synthesis of Nanoparticles. *a). TiO_2 Nanoparticles.* Two different solutions were prepared. Solution 1 was prepared by mixing 10 mL of tetraisopropyl orthotitanate with 25 mL of ethanol and 2 mL of ethylenediamine as template under vigorous stirring. Solution 2 was composed of 3 mL HCl, 20 mL distilled water, and 10 mL ethanol. Then the solution 2 was slowly injected into solution 1 under 40−50 °C, stirred for about 4 h. The resultant sol (with acidic pH) was kept in 80 °C and was dried. The needle black-brown product was finally obtained and calcined at 700 °C for 8 h in air. A similar approach was reported by Karn and Srivastava.[19]

b). ZrO_2 Nanoparticles. Zirconium oxychloride ($ZrOCl_2$. $8H_2O$) was used as source of Zr. The starting solution was prepared by mixing metal salt solution with a solution of 1.5 gr urea and 9 mL NH_3 (25 wt %) at 60−80 °C and pH between 9 and 10. Then 1−2 gr nonyl phenol ethoxylate (20 mol) was added as surfactant to form nanoemulsions. The solution was kept at 80 °C for 4 h with the reflux. The solid product was washed with ethanol and then dried at 100 °C followed by calcination at 800 °C for 8 h in air. This technique was already suggested and applied by Thammachart et al.[20]

c). SiO_2 Nanoparticles. The technique for preparing SiO_2 Nanoparticles can be found in Cao et al.[21] $Si(OC_2H_5)_4$ or TEOS was used as source of Si. Twenty milliliters of TEOS was dissolved in a mixture of isopropyl alcohol and ethanol and stirred at 50 °C for about 1 h. To this solution, then, 5 mL ethylene diamine and 3 g citric acid were added. The obtained solution was hydrolyzed by HNO_3 65 wt % solution for 2 h with vigorous stirring, followed by refluxing for 24 h. The final sample was evaporated, filtered, washed and dried in 80−100 °C, and finally calcined in 560 °C for 8 h in air.

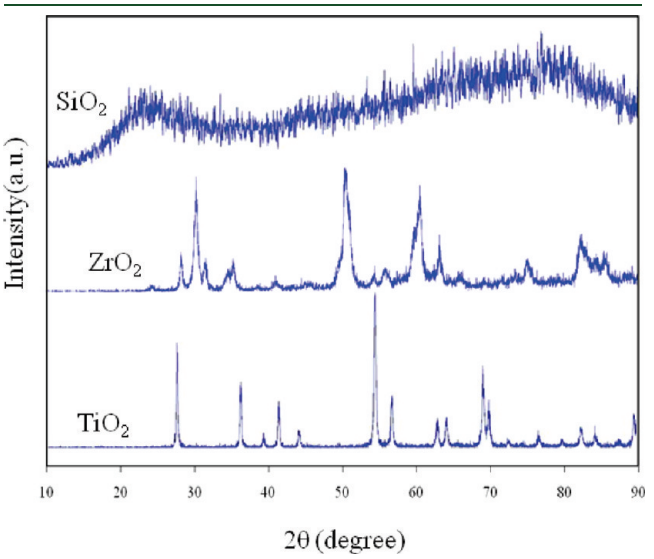

Figure 1. XRD patterns of rutile TiO_2, tetragonal ZrO_2 and an amorphous SiO_2 cristobalite, syn nanostructures.

2.2. Characterization of Nanopaticles. The XRD patterns and SEM images for the three nanoparticles are shown in Figures 1 and 2, respectively. The measured diffraction angles are reasonably consistent with the standard XRD profile of rutile TiO_2, tetragonal form of ZrO_2, and the amorphous phases of SiO2. The full-width-at-half-maximum (fwhm) of the XRD peaks from ZrO_2 is obviously broader than those of TiO_2, indicating the smaller sizes of the nano ZrO_2 particles than particles of TiO_2. The average crystallite size (t) for TiO_2 and ZrO_2 nanoparticles are calculated from Sherrer's Formula, given in eq 1

$$t = \frac{0.9\lambda}{\beta \cos\theta} \quad (1)$$

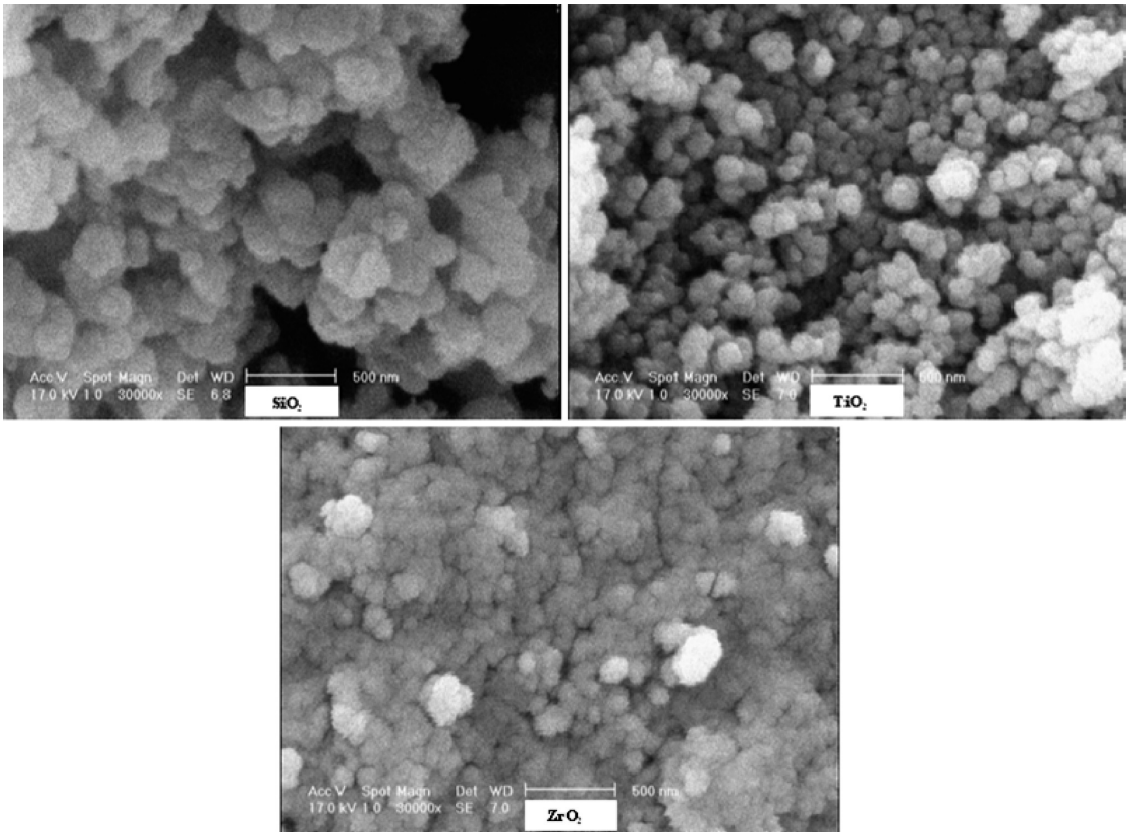

Figure 2. SEM images of SiO_2, TiO_2, and ZrO_2 as uniform nanospherical particles.

dx.doi.org/10.1021/ef2001635 |*Energy Fuels* 2011, 25, 3150–3156

where λ is the wavelength of X-ray radiation (1.548 Å for Cu Kα), β is the fwhm of the diffracted peak, and θ is the angle of diffraction. The maximum average crystallite size (t) for TiO_2 and ZrO_2 nanoparticles are calculated to be 15 and 9 nm, respectively. The SEM images presented in Figure 2 show uniform nanospherical particles for three types of nanoparticles.

2.3. Sample Preparation. Different nanofluids were prepared containing TiO_2, SiO_2, and ZrO_2 nanoparticles dispersed in paraffin (Merck, density 0.88 g/cm^3). All of the fluids were homogenized using ultrasonic homogenizer and their pH are adjusted by addition of HNO_3 or $C_2H_8N_2$ (ethylenediamine). Composition of nanofluids and their pH are given in Table 1. These samples are added to a crude oil taken from an Iranian oil reservoir to check their effect on the asphaltene stability. The oil has the API equal to 19 and contains about 10 wt % asphaltene. Each sample contains two grams of the crude oil, first centrifuged for 10 min at constant rotational speed of 3000 rpm to remove its solid particles, while mixed with 2 g of toluene for sample dilution. This fraction of the toluene considerably increases the solubility of asphaltene and makes the system highly stable. The final step is addition of 0.5 g of prepared nanofluids. Each final mixture contains 0.07 wt % of nanoparticle with the total volume of about 5 mL.

Table 1. Material Constituents Each Fluid and Nanofluid Samples[a]

samples	oil added fluids and nanofluids	pH
none		
P	Paraffin	
AP	Paraffin + HNO_3 (65%)	2
A	HNO_3 (65%)	
TP1	Paraffin + TiO_2 + HNO_3 (65%)	2
TP2	Paraffin + TiO_2 + $C_2H_8N_2$ (88%)	10
TP3	Paraffin + TiO_2	
TP4	Paraffin + TiO_2+ $C_2H_8N_2$ (88%)	8
ZP1	Paraffin + ZrO_2 + HNO3 (65%)	2
ZP2	Paraffin +ZrO_2 + $C_2H_8N_2$ (88%)	10
SiP1	Paraffin + SiO_2 + HNO_3 (65%)	2
SiP2	Paraffin + SiO_2+ $C_2H_8N_2$ (88%)	10

[a] The pH values are attributed to the solution of nanoparticles and acid and base before addition of the paraffin.

2.4. Experimental Procedure. All samples were titrated with *n*-heptane. Addition of *n*-heptane destabilizes asphaltene molecules or asphaltene nanoaggregates. In a certain concentration of *n*-heptane (called hereafter as onset), the nanoaggregates of asphaltene molecules cannot be dispersed stably in the bulk liquid phase and, therefore, precipitate as a separate phase. The titration procedure is performed by gradual and step-by-step addition of *n*-heptane. In each step, 1 cc *n*-heptane was added to the sample while stirring for 10 min. Then after, precipitation of asphaltene was investigated by a polarized-light microscope, model OLYMPUS BXP. The microscope has an upper lens with 10-fold magnification and a lower lens with 50-fold magnification. Its overall magnification is 500-fold. The procedure is explained in more detail elsewhere.[22−25] This procedure is repeated until all asphaltene molecules are precipitated, and the amounts of added *n*-heptane were determined for each sample. Figure 3 shows the typical microscopic results of different stages during the titration test for one of the samples.

2.5. Characterization of Precipitated Asphaltene. Fourier Transform Infrared (FTIR) Spectroscopy was used to study the type of functional groups present in *n*-heptane insoluble asphaltene corresponding to each sample. Infrared spectra are recorded using an FTIR spectrometer; model Bruker EQUINOX 55 in the absorbance mode with a spectral resolution of 0.96 cm^{-1} in the 4000−600 cm^{-1} spectral domain.

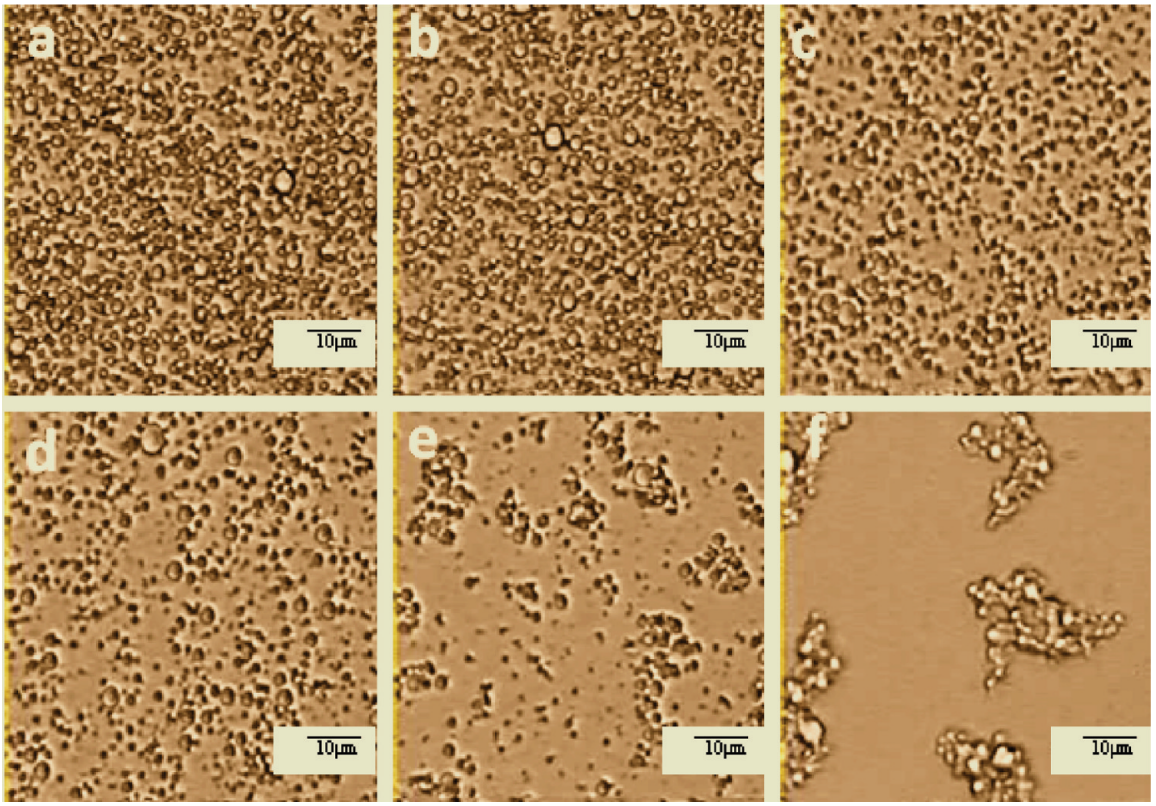

Figure 3. Micrographs of different stages of oil titration with *n*-heptane from (a) 0 cc added *n*-heptane to (f) 5 cc added *n*-heptane.

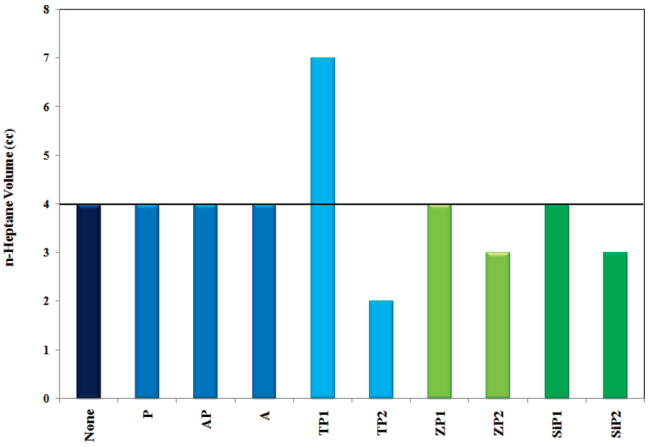

Figure 4. Onset point for asphaltene precipitation in terms of the required volume of *n*-heptane as precipitant. A deviation of ± 1 cm^3 must be considered for the onset points. The sample denoted by "None" is related to the crude oil with no added solvent. The constituents of the other solvents are listed in Table 1.

3. RESULTS AND DISCUSSIONS

To investigate the effect of nanoparticles in preventing asphaltene precipitation, the onsets of asphaltene precipitation were determined by polarized-light microscope for samples listed in Table 1. The micrographs for one of these samples (sample P) obtained by polarized-light microscopy are shown in Figure 3. As shown in the micrographs, the asphaltene particles are tiny at primary steps (panels a and b). By increasing the volume of added *n*-heptane the oil solution is diluted, until in onset point that the *n*-heptane insoluble particles are aggregated (panel e). After that, adding more *n*-heptane increases the sizes of aggregated asphaltenes (panel f).

Figure 4 compares the volume of *n*-heptane consumed up to the onset of asphaltene precipitation for different samples. Requiring more volumes of *n*-heptane implies more stability of asphaltene particles in oil. It is obvious from this figure that the sample, which contains TiO_2 nanoparticles in acidic conditions plays as asphaltene inhibitor, requiring about 7 cm^3 *n*-heptane for asphaltene precipitation.

As it is evident from this figure, addition of paraffin and acidic paraffin do not change the stability of asphaltene and have no impact on the onset of asphaltene precipitation. However, addition of TiO_2 nanoparticle to the system (sample TP1) strongly enhances the asphaltene stability and consequently increases the precipitation onset point. Changing the pH to basic conditions (sample TP2) reverses, interestingly and somehow expectedly, the fluid properties and causes precipitation of asphaltene in much lower values of added *n*-heptane. The reason for these observed phenomena can be seen in the interaction between TiO_2 and asphaltene in different pH conditions. To investigate the types of interactions between TiO_2 and asphaltenes at different pH conditions, we performed a FTIR test on the precipitated phase. The precipitated phase is first dried, being stored in 70 °C for three days, and used as solid phase for FTIR test.

The FTIR spectrum results of the precipitated asphaltene (the fraction insoluble in *n*-heptane) for samples of P, TP1, and TP2 are shown in Figure 5. The main differences between FTIR spectroscopy results for asphaltene of TP1 and two other samples are observed in the regions for O−H bond (3600−3100 cm^{-1}),

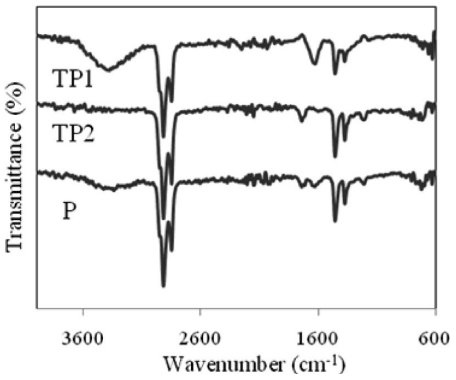

Figure 5. FTIR spectra of the precipitated phase in presence of the samples denoted as P, TP2, and TP1 in Table 1.

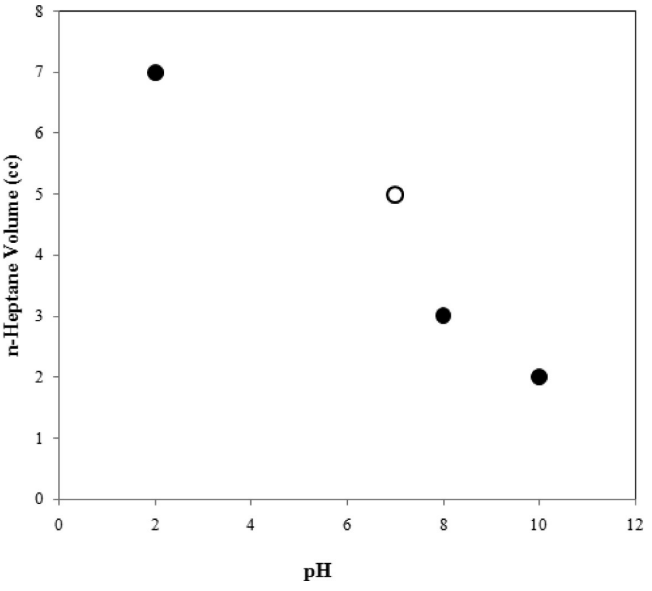

Figure 6. Onset of asphaltene precipitation points for samples with TiO_2 nanofluids versus pH. The open symbol is related to the sample denoted as TP3. Because TP3 is a nonaqueous system its pH has been assumed to be equal to 7 (not measured).

aliphatic C−H [(3100−2900 cm^{-1}) and (1500−1350 cm^{-1})], and aromatic C−H bonds(1700−1600 cm^{-1}), as identified and described by Calemma et al and Ibrahim and Idem.[26,27] The spectrum of TP1 indicates the presence of a broad −OH peak at (3600−3100 cm^{-1}), contrary to the other samples. According to Lopez et al, this peak occurs when Ti−OH bond is formed.[28] The intensity of absorbance for the aliphatic and aromatic functional groups in TP1 is different from those of other samples. The aliphatic peaks at (3100−2900 cm^{-1}) and (1500−1350 cm^{-1}) for TP1 is weaker than that for other samples, but the aromatic peak at (1700−1600 cm^{-1}) is a little stronger. These results imply that presence of TiO_2 nanoparticles in oil at acidic conditions can cause changes in the structure of *n*-heptane insoluble asphaltene parts and make the asphaltene system more stable. The strength of the hydrogen bond would be reduced in basic conditions and therefore less attachment would happen in higher pH (Figure 6). The observed hydrogen bond cannot be attributed to the bond between the protons of the acid and the oxygen atoms on TiO_2, for the sample has been fully dried (in 70 °C for 3 days) and used for

dx.doi.org/10.1021/ef2001635 |*Energy Fuels* 2011, 25, 3150–3156

Table 2. Samples prepared for DLS test. The concentration of asphaltene and TiO_2 nanoparticle in each sample is shown in brackets in grams per each liter of toluene

sample	materials	pH	aggregate size (nm)
A	Toluene + Asphaltene (0.2 gr/lit)		224
A1	Toluene + Asphaltene (0.2gr/lit) + HNO_3 (65%)	2	1890
N	Toluene + TiO_2 (0.2 gr/lit)		345
N1	Toluene + TiO_2 (0.2gr/lit) + HNO_3 (65%)	2	640
AN	Toluene + Asphaltene (0.1 gr/lit) + TiO_2 (0.1 gr/lit)		325
AN1	Toluene + Asphaltene (0.1 gr/lit) + TiO_2 (0.1 gr/lit) + HNO_3 (65%)	2	1160

the FTIR test in solid form. In such conditions the only materials available in the system are asphaltene and TiO_2.

It must be noted that even the interaction between asphaltene molecules can be in form of hydrogen bond formation. This idea has been verified by methylation of asphaltene.[29] In that, the hydrogen bonding sites, acidic hydrogen, has been substituted with a methyl group without affecting the hydrocarbon structure. It has been shown that methylation of asphaltene can lead to a decrease in viscosity of asphaltene solutions.[29] Figure 5 also shows a small bump in the region around 3200 cm^{-1} for the sample P, indicating hydrogen bond formation in this system. However, this peak is very small in comparison with the one observed in sample TP1. In other words, although asphaltenes can self-associate through hydrogen bonding, they can more favorably interact with other species like TiO_2 in similar way.

To support the above results, we have moreover performed a dynamic light scattering (DLS) measurement to measure the sizes of the nanoaggregates of asphaltenes in presence of TiO_2 particles at different pH conditions. In that, if the occurrence of hydrogen bond is the case in acidic conditions, the sizes of aggregates must be much higher than those at higher pH. The DLS tests are performed making use of Nonosizer-ZS (Mastersizer, Malvern Instruments, Worcestershire, UK), equipped with a Helium−Neon laser (633 nm) using disposable cuvette. For this reason, we extracted the asphaltenes from the crude oil. To extract the asphaltene from the crude oil, centrifuged crude oil was mixed with *n*-heptane at a volume ratio of 1:40. The mixture was stirred with magnetic stirrer for 24 h, and then the insoluble materials (including asphaltene) were separated by centrifugation and were dissolved in toluene and the solution was centrifuged again to separate toluene insoluble materials. At the end, the solution was dried and the asphaltene powder was obtained.

Six samples were prepared, shown in Table 2, for DLS measurement. Sample A contains 0.2 gr of the above obtained asphaltene per liter of toluene. According to the DLS results for this sample, there is a wide range of aggregate sizes ranging from 50 nm to about 3 μm. Most of the aggregates, however, are of the order of 100 nm and the average value is found to be 224 nm (Figure 7). It is established that dilute toluene solutions of asphaltenes exhibit nanoaggregate formation at a certain asphaltene concentration, known as critical nanoaggregate concentration (CNC).[29] However, different asphaltenes exhibit different CNCs. A range of values between 50 to 150 mg/L has been reported in the literature for the CNC of some asphaltenes.[29] The sizes of the nanoaggregates also are reported to vary from

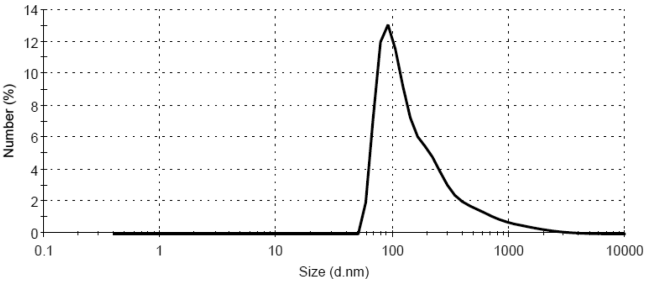

Figure 7. Particle size distribution in system denoted as A in Table 2.

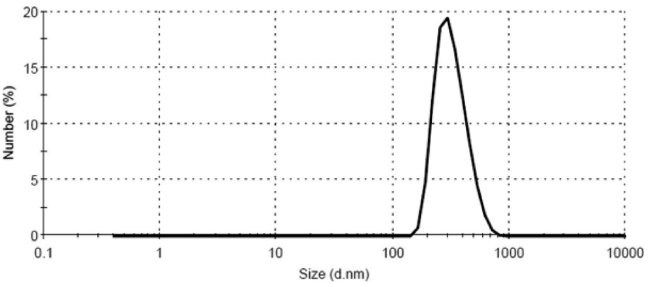

Figure 8. Particle size distribution in system denoted as AN in Table 2.

1.5 nm to about 100 nm. Our measurement shows that most of the particles are in the similar range. Existence of large size particles may be due to the concentration of asphaltene (200 mg/L) which can be considerably higher than the CNC. The average size, however, increases sharply to 1890 nm by lowering the pH to 2; using small amounts of HNO_3 (sample A1 in Table 2). It is also indicated from DLS data that no particle below micrometer size is available in this condition. These data reveal the tendency of asphaltenes to get aggregated in acidic conditions. Considering the average sizes in both systems we can conclude that about 8−9 particles are aggregated to form bigger aggregates at acidic conditions.

Sample N contains 0.2 gr of TiO_2 nanoparticles per each liter of toluene. The DLS data shows an average value of 325 nm for this system. Similar to sample A1, addition of HNO3 and changing the pH to more acidic conditions results in the aggregation of the nanoparticles (sample N1) with an average size of about 640 nm. This implies that about two particles are attached to form the new aggregates. Considering the aggregation numbers in samples A1 and N1, it seems that asphaltenes have much higher tendency to get aggregated at acidic conditions than TiO_2 nanoparticles.

Addition of asphaltene to the sample N results in small reduction in the average size of the available aggregates in the system (sample AN). This fact implies no aggregation between asphaltene and TiO_2 nanoaggregates in this condition. The measured distribution of sizes also reveals that particles as small as 200 nm and as big as 1 μm are available in the system (Figure 8). The average value is found to be 325 nm. Also, according to FTIR data, there is no chemical bond between TiO_2 and asphaltene when pH is not sufficiently low.

Addition of asphaltene to sample N1 results in considerable increase in the average size of the available aggregates in the system (sample AN1). The size distribution data, Figure 9, indicate availability of no or negligible particles below 800 nm

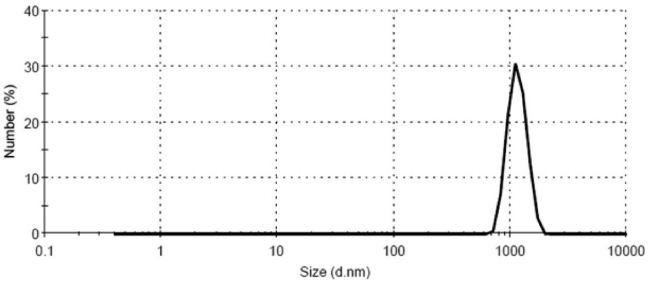

Figure 9. Particle size distribution in system denoted as AN1 in Table 2.

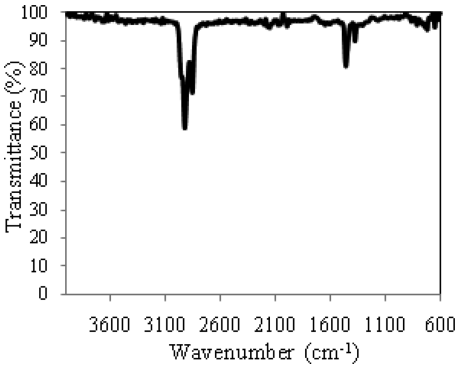

Figure 10. FTIR spectrum of the precipitated phase in presence of the sample denoted as SiP1 in Table 1.

and above 2 μm. In another words, there is no free TiO_2 nanoaggregates (average size of 640 nm in sample N1), and also there is no or negligible free asphaltene aggregates (average size of 1890 nm in sample A1). Therefore, almost all of the TiO_2 particles are attached to asphaltenes to form new aggregates, mostly with the size of 1160 nm. It must be noted that at acidic conditions no asphaltene aggregates could be found below 1 μm in sample A1. These data along with the FTIR results, although not rigorously, support the occurrence of hydrogen bonding between TiO_2 and asphaltene in low pH.

Nanofluids ZP1, ZP2, SiP1, and SiP2 are those containing nanoparticles of SiO_2 and ZrO_2 in two different pH values. Onset points for the acidic nanofluids (SiP1 and ZP1) are found equal with the original crude oil with no enhancement in asphaltene stability. However, in higher pH (SiP2 and ZP2), onset points are lower than acidic ones. The FTIR spectrum obtained for the precipitated phase in presence of SiP1, Figure 10, shows similar trend as samples of P and TP2, indicating that no chemical bonding has been occurred in such system.

4. CONCLUSIONS

In this work, impacts of TiO_2, SiO_2, and ZrO_2 nanoparticles on asphaltene stability of an Iranian crude oil were investigated at different pH regions. The onset of asphaltene precipitation was measured for each sample. It is observed that the nanofluids cannot act as asphaltene precipitant in strongly acidic conditions, and, moreover, they may play as a dispersant, enhancing the stability of the asphaltene. In the case of nanofluids containing TiO_2 nanoparticles at acidic conditions, we found that TiO_2 nanoparticles enhances stability of asphaltene in the fluid, hence a higher precipitation onset point. On the basis of the experimental results and observations, this is the result of a hydrogen bond formed between asphaltene and TiO_2 nanoparticles, as verified by FTIR and DLS data.

AUTHOR INFORMATION

Corresponding Author

*E-mail: abahram@ut.ac.ir; Tel: +982161114715; Fax: +982188632976.

ACKNOWLEDGMENT

This work is supported by NIOC-R&D (Contract No. 81-88009), which is gratefully acknowledged. We do also thank M. Sadeghi Naeini and R. Hosseini for their considerable help with the experiments.

REFERENCES

(1) Aske, N.; Kallevik, H.; Johnsen, E. E.; Sjöblom, J. *Energy Fuels* **2002**, *16* (5), 1287–1295.

(2) Pedersen, K. S.; Christensen, P. L. *Phase Behavior of Petroleum Reservoir Fluids*; CRC Press: Boca Raton, FL, 2007.

(3) Thawer, R.; Nicoll, D. C. A.; Dick, G. *SPE Prod. Eng.* **1990**, *5*, 475–480.

(4) Valter Antonio, M. B.; Mansoori, G. A.; De Almeida Xavier, L. C.; Park, S. J.; Manafi, H. *J. Pet. Sci. Eng.* **2001**, *32*, 217–230.

(5) Barcenas, M.; Orea, P.; Buenrostro-González, E.; Zamudio-Rivera, L. S.; Duda, Y. *Energy Fuels* **2008**, *22*, 1917–1922.

(6) Ghloum, E. F.; Al-Qahtani, M.; Al-Rashid, A. *J. Pet. Sci. Eng.* **2010**, *70*, 99–106.

(7) Laux, H.; Rahimian, I.; Butz, T. *Fuel Process. Technol.* **2000**, *67*, 79–89.

(8) Oh, K.; Deo, M. D. *Energy Fuels* **2002**, *16*, 694–699.

(9) Chang, C.-L.; Fogler, H. S. *Langmuir* **1994**, *10* (6), 1758–1766.

(10) Kraiwattanawong, K.; Scott Fogler, H.; Gharfeh, S. G.; Singh, P.; Thomason, W. H.; Chavadej, S. *Energy Fuels* **2009**, *23*, 1575–1582.

(11) Mukkamala, R. U.S. Patent 7,097,759, 2006.

(12) Permsukarome, P.; Chang, C.; Fogler, H. S. *Ind. Eng. Chem. Res.* **1997**, *36* (9), 3960–3967.

(13) Wilkes, M. F.; Davies, M. C. U.S. Patent Application 2008/0096772, 2008.

(14) León, O.; Contreras, E.; Rogel, E. *Colloids Surf., A* **2001**, *189*, 123–130.

(15) Yudin, I. K.; Nikolaenko, G. L.; Kosov, V. I.; Melikyan, V. R.; Markhashov, E. L.; Frot, D.; Briolamt, Y. *J. Pet. Sci. Eng.* **1998**, *20*, 297.

(16) Skauge, T.; Spildo, K.; Skauge, A. Nano-sized particles for EOR. In *17th SPE Improved Oil Recovery Symposium*, Society of Petroleum Engineers (SPE), 2010; Vol. 2, pp 1281−1290.

(17) Fletcher, A. J. P.; Davis, J. P. How EOR can be transformed by nanotechnology. In *17th SPE Improved Oil Recovery Symposium 2010*, Society of Petroleum Engineers (SPE), Tulsa, Oklahoma, USA, 2010; Vol. 1, pp 152−167.

(18) Wang, K.; Liang, S.; Wang, C. Research of improving water injection effect by using active SiO 2 nano-powder in the low-permeability oilfield. In *2009 China International Powder Technology and Application Forum*, Trans Tech Publications, March 30; Vol. 92, pp 207−212.

(19) Karn, R. K.; Srivastava, O. N. *J. Hydrogen Energy* **1998**, *23*, 439–444.

(20) Thammachart, M.; Meeyoo, V.; Risksomboon, T.; Osuwan, S. *Catal. Today* **2001**, *68*, 53–61.

(21) Cao, Y.; Dai, W. L.; Deng, J. F. *Mater. Lett.* **2001**, *50*, 12–17.

(22) Wilson, A. D.; Boek, E. S.; Ladva, H. K.; Crawshaw, J.; Padding, J. T., Recent Developments in the Deposition of Colloidal Asphaltene in Capillary Flow: Experiments and Mesoscopic Simulation. In *8th European Formation Damage Conference*, Society of Petroleum Engineers (SPE), Scheveningen, The Netherlands, 2009.

(23) Hung, J.; Castillo, J.; Reyes, A. *Energy Fuels* **2005**, *19*, 898–904.
(24) Buckley, J. S. *Petrol. Sci. Technol.* **1996**, *14* (1&2), 55–74.
(25) Wang, J. X.; Brower, K. R.; Buckley, J. S. *SPE Journal* **2000**, *5* (4), 420–425.
(26) Calemma, V.; Iwanski, P.; Nali, M.; Scotti, R.; Montanari, L. *Energy Fuels* **1995**, *9*, 225–230.
(27) Ibrahim, H. H.; Idem, R. O. *Energy Fuels* **2004**, *18*, 1354–1369.
(28) Lopez, T.; Sanchez, E.; Bosch, P.; Meas, Y.; Gomez, R. *Mater. Chem. Phys.* **1992**, *32*, 141–152.
(29) Mullins, O. C.; Sheu, E. Y.; Hammami, A.; Marshall, A. G. *Asphaltenes, Heavy Oils, and Petroleomics*; Springer: New York, 2007.